Physica D 309 (2015) 9–19

Contents lists available at ScienceDirect

Physica D

journal homepage: www.elsevier.com/locate/physd

Detecting changes in coupling with Granger causality method from time series with fast transient processes

Ilya V. Sysoev [a,b,*], Marina V. Sysoeva [c,b]

[a] Saratov State University, 83, Astrakhanskaya str., Saratov, Russia
[b] Saratov Branch of Institute of Radioengineering and Electronics of RAS, 38, Zelenaya str., Saratov, Russia
[c] Yuri Gagarin State Technical University of Saratov, 77 Politechnicheskaya street, Saratov, 410054, Russia

HIGHLIGHTS

- To study non-stationary time series the Granger causality must be adapted to data.
- The instant of the evolution operator change can be found using the adapted method.
- One can detect if the oscillation properties changed due to the coupling or not.

ARTICLE INFO

Article history:
Received 21 July 2014
Received in revised form
24 April 2015
Accepted 10 July 2015
Available online 26 July 2015
Communicated by T. Sauer

Keywords:
Coupling detection
Granger causality
Non-stationary time series
Non-linear models
Transient processes
Surrogate time series

ABSTRACT

The ability of the Granger causality method to detect directed coupling between subsystems of a complex system in a moving time window is investigated on etalon oscillators. In particular, the time series consisting of alternate stationary regimes characterised by the different amplitude and shape of oscillations with fast transient processes between these regimes are considered, with similar transitions being possible due to changes either in the coupling or in the individual properties of subsystems. Two popular approaches to surrogate times series generation are used to check the significance of the method results. Two model structures: the standard linear and the special non-linear adapted to data are implemented.

The Granger causality method using the model structure adapted to data is shown to be significantly advantageous in detecting coupling directionality and the instant time of the regime change than the standard linear method, while in some cases the sensitivity and the specificity of the adapted approach are insufficient.

1. Introduction

Investigation of transition from one typical regime to another in complex systems, composed from a number of subsystems, is a fundamental task, because such systems are a corner-stone of modern scientific conceptions. For instance, brain is considered to be composed of large parts: cortex, cerebellum, thalamus, hippocampus, etc., which consist of smaller areas such as different thalamic nuclei or cortical layers. Another example is the Earth climate, which is considered to be composed of individual, but related phenomena such as El-Niño and the North-Atlantic oscillation.

The evolution of such complex systems is commonly observed through measurement of time series from its subsystems. Through measuring the signals of individual subsystems one can try to find out whether the changes in a complex system are result of the changes in individual properties of its subsystems, or they occur due to the changes in the coupling between different subsystems. To answer this question one can use the existing methods based on construction of empirical forecasting models, which are adapted to work in a moving time window. These methods are actively applied in the neurophysiology [1–5] and climatology [6,7]. Among the most popular are the different kinds of Granger causality technique [8–11], information based measures [12,13], a partial directed coherence [14], and approaches based on modelling phase dynamics [15,16]. The main idea of these approaches is similar, and in some cases they can be shown to be completely equal [17].

The time varying Granger causality [18] seems to be very promising for the investigation of non-stationary time series of complex systems due to its significant advantages. First, it allows to determine the coupling directionality, which is not possible with simple measures such as correlation function, coherency function and mutual information. Second, Granger causality demands the

* Corresponding author at: Saratov State University, 83, Astrakhanskaya str., Saratov, Russia.
E-mail addresses: ivssci@gmail.com (I.V. Sysoev), bobrichek@mail.ru (M.V. Sysoeva).

http://dx.doi.org/10.1016/j.physd.2015.07.005
0167-2789/

series of less length (both in number of data points and in number of oscillations) than the transfer entropy or the phase dynamics methods. This fact makes it possible to analyse the coupling in a comparatively short moving time window, so the dependency of the coupling on time can be estimated.

The approaches proposed in [19–21] are advantageous in comparison with the pairwise techniques since they can distinguish between the direct and mediate coupling if all the necessary signals are provided. However, these methods demand a lot of data and are not very suitable for the short and non-stationary series because a large number of coefficients has to be estimated. To decrease the model dimension, and consequently the number of coefficients in [22] it was proposed to use only the primary variables rather than all measured ones (transfer entropy estimates were considered). The principle problem of multivariate techniques is that all variables, considered to make a significant impact on the network dynamics, have to be measured. If some of them are hidden, which often occurs in real experiments (e.g. in the neurophysiology a lot of brain areas are anatomically connected), distinguishing between a directed and a mediate coupling becomes unreliable.

The main shortcoming of the Granger causality approach in application to the task of diagnostics of time-related changes in complex system is that it is heavily based on model construction, therefore time series are assumed to be stationary, at least for a length of a moving window. In some recent applications of the methods similar to Granger causality to the neurophysiology [23,24] the improved dual Kalman filter is combined with the renormalised partial directed coherence (that can be treated as a Granger causality resolved in the frequency domain) and linear phase space modelling to assess the coupling varying in time. In general, such an approach is declared to be applicable to non-linear, non-stationary noisy data of arbitrary nature. However, the practical evidence of that is not completely clear, since originally [24] its efficiency was demonstrated on 4 coupled autoregressive processes of first order with additive Gaussian noise.

The transfer entropy and the partial directed coherence became so popular in comparison with the straightforward Granger causality approach (as implemented in [9,10,25]) due to the heavy dependence of this straightforward approach on the structure of the model and on a choice of the type and the number of non-linear functions. However, this problem can be at least partially solved using statistical criteria to choose polynomial order (or number and type of other basis functions) and model dimension (e.g. Schwarz criterion [26] (BIC) or Akaike criterion [27]), and taking into account signal properties, while constructing state vector, as it was demonstrated in [28]. So, in order to apply Granger causality to experimental data, it is important, first, to understand, how the non-stationarity of an investigated series can affect the method efficiency. This task is divided into two: to measure method sensitivity to changes in parameters of individual subsystems, and to measure its sensitivity to changes in coupling between them. The first step to this task solution can be done by investigating the series with fast transient processes, separating relatively long stationary stages. The investigation of applying the Granger causality to such series is the goal of the current paper.

In the frames of the formulated goal, the following questions were addressed in the numerical experiment using specially constructed etalon systems:

1. Does the method always detect coupling directionality? E.g. can it show the coupling to be bidirectional, when is it really unidirectional?
2. In what situation can the method sensitivity be insufficient, e.g. due to the inappropriate account of non-linearity, as it was previously mentioned in [9,29]?
3. Usually surrogate time series are constructed to estimate the significance level of achieved results. How can an approach to surrogates construction affect the method results?
4. How does the method perform with an increase of synchrony level between considered time series? Does it allow to distinguish between situations when the synchrony is a result of an interaction, and when it occurs due to some random factors? Is it possible to understand whether the synchronisation is a result of unidirectional or bidirectional interaction?
5. What is the time resolution of Granger causality coupling estimates? How does the Granger causality method perform, when changes in the individual characteristics, such as mean or variance, delay comparatively to changes in coupling?
6. Can the method distinguish between the same changes in the signal shape and amplitude caused by changes either in the coupling or in individual parameters of subsystems?

Formulated issues are very complex and general, and they cannot be solved within the single work. Therefore we only try to perform an example of an investigation for a certain class of systems and signals in order to reveal the most common method features.

In order to realise the potential advantages of the Granger causality method, one should be very careful with the choice of used models and has to take into account the specifics of experimental data even for stationary series. For instance, an insufficient account of non-linearity leads to a loss in the sensitivity [9,29], too low sampling rate [30], observation noise [31] and an inadequate consideration of the time scales of observed series [32] lead to false positive results, redundant variables lead to underestimation of coupling strength, while synergetic ones—to overestimation [33]. However, sometimes even the most simple models are enough to reveal the coupling, as shown in [3], and the qualitative reproduction of the observed dynamical regime is not necessary to succeed [34], as well as linear models can reveal a coupling between non-linear systems [35]. Therefore two versions of the straightforward Granger causality approach were considered: the standard linear algorithm (as regarded in many papers, e.g. [3,5]) and the adapted method developed in [28] in application to the problem of the coupling estimation between the different brain structures for WAG/Rij epileptic rats.

2. The etalon oscillators and the investigation technique

Oscillators which are well known in non-linear dynamics were decided to be used as subsystems. They were modified to demonstrate two different regimes: irregular oscillations with a low amplitude (*regime* 1) and more regular oscillations with a higher amplitude (*regime* 2). Coupling was implemented in a special manner to provide a possibility to switch between these regimes either by changing individual parameters of subsystems or by changing coupling intensity, while both of these ways lead to the same changes in shape and amplitude of oscillations. Ensembles of up to four subsystems were considered.

The etalon oscillator of the first type was a stochastic oscillator with a threshold excitation (a variation of the van der Pol oscillator) with a Toda potential (1):

$$\frac{dx_i}{dt} - \left(r_i - x_i^4 + k_i(t)x_j^2\right)\frac{dx_i}{dt} + 1 - e^{-x_i} = \xi_i(t), \tag{1}$$

where i is a current oscillator number, j is a driving oscillator number, $k_i(t)$ is a variant in time coupling coefficient, r_i is a coefficient of non-linearity, and $\xi_i(t)$ is a realisation of normal white noise. Coefficients $r_i \in [-0.14; -0.07]$ $\forall i$, which correspond to a stable fixed point attractor in absence of noise.

The etalon oscillator of the second type was a stochastic Rössler oscillator:

$$\begin{aligned}\dot{x}_i &= -y_i - z_i,\\ \dot{y}_i &= x_i + a_i y_i,\\ \dot{z}_i &= b_i - z_i\left(c_i - x_i - 2.5k_i z_j\right) + \xi(t),\end{aligned} \tag{2}$$

with i, j, and ξ having the same meaning, and a_i, b_i, and c_i being individual subsystem parameters chosen to demonstrate a periodic regime with low amplitude oscillations: $a_i = 0.2$, $b_i \in [0.12; 0.2]$, $c_i \in [2.6, 3.2]$.

Subsystems of two types were used to make the achieved results more general, since the subsystems (1) and (2) have different dimensions and demonstrate different dynamics with default coefficients and zero coupling: under-threshold oscillations induced by the noise for subsystems of type (1), and regular oscillations for subsystems of type (2). It is important that oscillators (2) can show latency in the oscillation amplitude and shape change when switching regimes (see Fig. 1). The problem of the correspondence lack between a change in parameters and a change in oscillation characteristics was already discussed, e.g. in [36], and it is very important in practice. One needs to know whether the method allows to reveal a time moment of an actual change in the coupling or self parameters of individual subsystems, or it can only provide an information that some statistical properties of a regime such as a variance or an oscillation shape have changed.

All the considered etalon systems were solved numerically with sampling rate 0.08. Then for the convenience of a further consideration the arbitrary time was introduced with setting 1 s = 1024 sampling points. Time series of the x coordinate for both subsystem types were recorded and analysed. The whole series length was equal to 30 s. In all cases each oscillator with an index i was driven by the only oscillator with an index j, with the coupling architecture being different in order to test different hypotheses.

Series were divided into three stages. The first one (seconds 0–10, i.e. the first 10 240 values) and the third one (seconds 20–30, i.e. the last 10 240 values) corresponded to the regime 1 with zero (or low) coupling $k = 0$ (or $k = 0.01$), with other coefficients being set to their default values. It has to be mentioned that the individual time series characteristics, such as the probability density, the power spectrum, and the autocorrelation function for very low coupling ($k = 0.01$) were found to be statistically not different (e.g. based on Kolmogorov–Smirnov test for probability density) from the same characteristics in zero coupling case. The coupling analysis, described further, also did not show the difference between low and absent coupling. The main reasons for this were high level of the noise and the relatively small length of the considered time window (1024 points and only about 8 oscillations). Therefore these cases of the low coupling and the zero coupling were addressed here together as uncoupled.

The second stage (the central one, i.e. seconds 10–20) corresponded to the regime 2 and was obtained either by increasing the coupling coefficient to the value $k = 0.65$, or by changing the individual parameters of the subsystems from their default values: r_i for (1) and c_i for (2). If more than 2 subsystems were considered, all k_i were set to be equal. During transient processes the coefficients k_i were increased or decreased smoothly but fast with a step $\Delta k = 0.001$ per 1/8192 s. Coefficients of individual subsystems were changed similarly. If the regime 2 was obtained by changing the individual parameters of subsystems, the coupling could remain either low ($k = 0.01$) or zero. No difference was found between these cases. For each considered coupling architecture an ensemble of 100 sets of realisations was considered, with each realisation set generated under the individual random initial conditions and using an independent realisation of the noise. The analysis of such a large ensemble was performed to provide the statistical reliability to the achieved results.

In all the cases Granger causality was calculated in a moving window of length 1 s (1024 data points) with a time shift 0.1 s. Such an approach is known in literature as "time-variant Granger causality" [18].

To answer the questions, formulated in the *Introduction* section, the large number of numerical experiments was performed. Particularly, for the questions 1 and 2 the detailed investigation of ensembles with the different coupling architecture was done (see Section 4).

To answer the question 3 two popular approaches to surrogate series generation [37] were used in all numerical experiments. The first one is a randomisation of phases of components of the Fourier transform. In this case, first, the direct Fourier transform of a signal was performed, then the amplitudes of an obtained Fourier image were kept, while its phases were set to be random numbers uniformly distributed in the semi-interval $[0;\ 2\pi)$, and then a surrogate series was calculated as an inverse Fourier transform. This was repeated in each numerical experiment 100 times with different random phases to obtain 100 surrogate time series. The second approach was a permutation of different realisations from the measured ensemble. This meant that for each investigated pair of realisations 100 surrogate pairs were randomly composed of other realisation pairs. Since signals in these surrogate pairs were taken from different realisations, they were not coupled, but they still kept the individual properties of the investigated processes, such as a distribution density and a power spectrum. Though these approaches actually address different null hypotheses, they are widely used for coupling detection.

To answer the question 4 a method to detect synchrony has to be used. Since the full synchronisation obviously prevents any attempts to find the coupling direction, only a partial synchronisation should be considered. For oscillatory signals with a characteristic time scale the phase synchronisation seems to be the most important. Therefore the phase synchronisation index was calculated as it was mentioned in [38]:

$$\Phi_{x,y} = \left|\left\langle \exp\left(i(\phi_x - \phi_y)\right)\right\rangle_{n=1,\ldots,N}\right|, \tag{3}$$

where N is a number of points in a series or in its fragment, ϕ_x and ϕ_y are phases of investigated signals. If the phase difference between signals is fixed in time (the phase synchronisation occurs), then $\Phi_{x,y} = 1$. If the phase difference is uniformly distributed in semi-interval $[0; 2\pi)$, i.e. all possible values of the phase difference are equally probable (no phase synchrony), then $\Phi_{x,y} = 0$.

For all considered cases the phase synchronisation index was estimated in the moving window of the same length as the one used for the Granger causality calculation. Its 95% confidence interval was also estimated from its own surrogate series constructed separately for each time window by randomising components of the Fourier transform.

3. Granger causality method

Let there be two objects: the object X from which the time series $\{x\}_{n=1}^{N}$ is obtained, and the object Y from which the time series $\{y\}_{n=1}^{N}$ is obtained. The study of causal interactions between X and Y with the Granger causality method includes three steps.

First, a univariate predictive model is constructed from the time series $\{x_n\}_{n=1}^{N}$, e.g. in the form of model map (4).

$$x'_{n+\tau} = f\left(x_n, x_{n-l}, \ldots, x_{n-(D_s-1)l}\right), \tag{4}$$

where $\mathbf{x}_n = \left(x_n, x_{n-l}, \ldots, x_{n-(D_s-1)l}\right)$ is a state vector reconstructed by means of the method of delays [39], the components of which are obtained from the same observable time series by shifting it back in time by an interval of l time points $(D_s - 1)$ times;

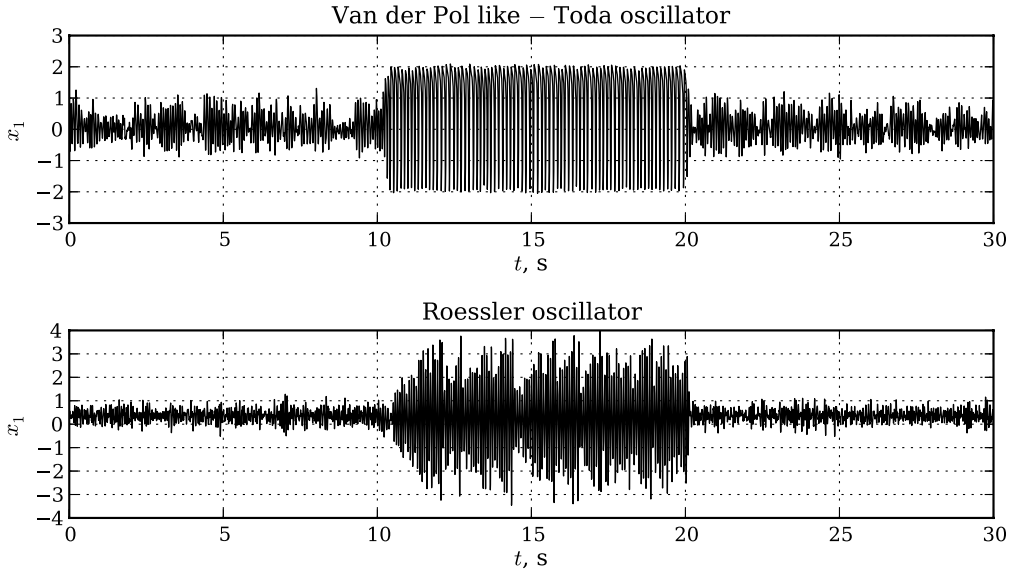

Fig. 1. Time series of etalon oscillators (1) and (2).

l is a time delay (or lag), and D_s is a univariate model dimension that is actually the number of components in the reconstructed state vector $\{\mathbf{x}_n\}_{n=1}^{N-(D-1)l}$; x'_n is a predicted value corresponding to a measured value x_n, τ is a length of the prediction interval (the prediction length), i.e. the time in data points between the last point used for state vector reconstruction and the predicted point. Model coefficients are estimated using the least-squares routine [40] by minimising the squared prediction error (5), that measures the difference between the predicted values $x'_{n+\tau}$ and the observed ones $x_{n+\tau}$:

$$\varepsilon_s^2 = \frac{1}{N'\sigma_x^2} \sum_{n=(D_s-1)l}^{N-\tau} \left(x'_{n+\tau} - x_{n+\tau}\right)^2 \to \min \tag{5}$$

where σ_x^2 is the variance of the time series $\{x_n\}_{n=1}^N$, $N' = N - \tau - (D_s - 1)l$ is the efficient length of the time series.

Second, a bivariate model (6) is constructed from both time series $\{x_n\}_{n=1}^N$ and $\{y_n\}_{n=1}^N$:

$$x''_{n+\tau} = g\left(x_n, x_{n-l}, \ldots, x_{n-(D_s-1)l}, y_n, \ldots, y_{n-(D_a-1)l}\right), \tag{6}$$

where D_a is a dimension of the state vector $\mathbf{y}_n = \left(y_n, y_{n-l}, \ldots, y_{n-(D_a-1)l}\right)$ reconstructed from the scalar time series $\{y_n\}_{n=1}^N$ in (6). So the total dimension of the bivariate model can be computed as $D_j = D_s + D_a$, and its prediction error is denoted as ε_j^2.

Third, the value of the *prediction improvement* PI (7), that is considered as a main characteristic of the Granger causality method, is computed.

$$PI = 1 - \frac{\varepsilon_j^2}{\varepsilon_s^2}. \tag{7}$$

The equality of ε_j^2 and ε_s^2 suggests that taking into account the time series $\{y_n\}_{n=1}^N$ cannot improve the prediction of $\{x_n\}_{n=1}^N$. In other words, Y does not drive X. A situation when $\varepsilon_s^2 > 0$ and $\varepsilon_j^2 \to 0$, providing $PI \to 1$, suggests that the data from $\{y_n\}_{n=1}^N$ exceedingly improve prediction of $\{x_n\}_{n=1}^N$, so Y is said to drive X.

The outcomes of the Granger causality method depend on model parameters, such as a type of basis function [9,10], their number (in our case—polynomial order [29,34]), the time lag and the prediction length [32]. Since these parameters are crucially important for the practical application of the Granger causality method, they have to be carefully chosen to achieve reliable results.

When applying Granger causality, the most often used models are standard linear of type (8) like in [3], with the time lag and the prediction length being equal to one sampling interval, and the only optimised parameters being dimensions D_s and D_a. This optimisation is usually done based on the prediction error saturation criterion (see, for example, [41]). However, it is often hard to think out, with what values of D_s and D_a the saturation occurs. Therefore the Bayesian information criterion (BIC) [26] was used to determine the dimension D_s. $D_s = 7$ was found to be optimal for subsystems of type (1) and $D_s = 6$ was found to be optimal for subsystems of type (2). $D_a = 1$ was chosen for both types of subsystems to prevent the increase in the number of false positive results.

$$\begin{aligned} x'_{n+1} &= c_0^s + \sum_{i=1}^{D_s} c_i^s x_{n-(i-1)}, \\ x''_{n+1} &= c_0^j + \sum_{i=1}^{D_s} c_i^j x_{n-(i-1)} + \sum_{i=D_s+1}^{D_s+D_a} c_i^j y_{n-(i-D_s-1)}, \end{aligned} \tag{8}$$

where c_i^s are empirically fitted coefficients of the univariate model and c_i^j are coefficients of the bivariate model.

However, it was shown that non-linear models may provide the significantly better sensitivity [9,10,29]. Our investigations in [42] were aimed at developing the adapted to data non-linear model (see (9)).

$$x'_{n+\tau} = \sum_{k=0}^{P} \sum_{q=1}^{C_{D_s+k}^k} c_i^s \prod_{m=1}^{D_s} x_{n-(m-1)l}^{w_{k,m}^s} + c_{Z_s+1} x_{n-l_T}, \tag{9a}$$

$$\forall k = 0, \ldots, P \sum_{m=1}^{D_s} w_{k,m}^s = k$$

$$\begin{aligned} x''_{n+\tau} = &\sum_{k=0}^{P} \sum_{q=1}^{C_{D_s+D_a+k}^k} c_i^j \prod_{m=1}^{D_s} x_{n-(m-1)l}^{w_{k,m}^j} \prod_{m=1}^{D_a} y_{n-(m-1)l}^{w_{k,(m+D_s)}^j} \\ &+ c_{Z_j+1} x_{n-l_T} + c_{Z_j+2} y_{n-l_T} \end{aligned} \tag{9b}$$

$$\forall k = 0, \ldots, P \sum_{m=1}^{D_s+D_a} w_{k,m}^j = k,$$

where $Z_s = (P + D_s)!/(P!D_s!)$ is the number of coefficients in the univariate model (9a), $Z_j = (P + D_s + D_a)!/(P!(D_s + D_a)!)$

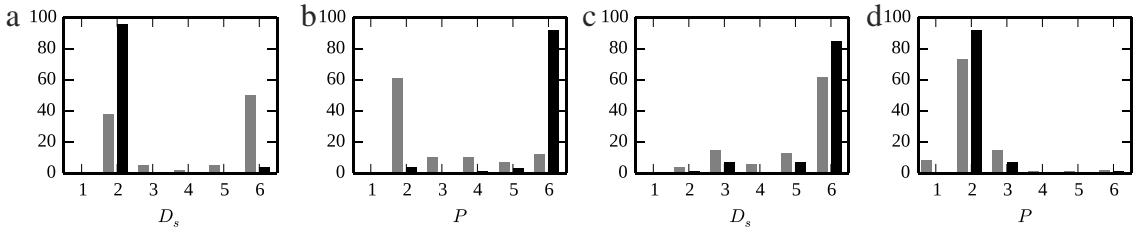

Fig. 2. The histogram of distribution of the dimension D_s and the polynomial order P for subsystems of the type (1) (a, b) and of the type (2) (c, d). The grey bars correspond to the stage 1, while the black ones correspond to the stage 2.

is the number of coefficients in the bivariate model (9b), $C^k_{D_s+k}$ is the number of combinations varied from $D_s + k$ to k, P is the polynomial order, l_T is the additional lag that takes into account the value of the experimental data delayed from the predicted one on a characteristic period T. This approach is known as a non-uniform embedding procedure (see [43]) and it was used in [13]. Together with determining the best dimension D_s and the polynomial order P based on BIC it solves the problem of reducing the model size. The BIC was calculated for the stages 1 and 2 (stage 3 is equivalent to the stage 1) separately for both types of subsystems for all 100 realisations using the 1 s (1024 points) window (3rd and 13th seconds of realisations were used). The distribution of the obtained values for uncoupled systems is plotted in Fig. 2, while very similar distributions could be plotted for the unidirectionally and bidirectionally coupled ones. P and D_s were chosen based on the analysis of these distributions. For the oscillators of the type (1) the optimal values are different for the stages 1 and 2, we used the maximal polynomial order $P = 6$, since it is necessary for the stage 2, and the second most common value for $D_s = 2$, since using $D_s = 6$ with $P = 6$ leads to too many coefficients. For the oscillators of the type (2) the optimal values for both stages occurred to be the same: $P = 2, D_s = 6$. Such a choice is in a good correspondence with the fact, that originally the oscillator (1) is highly non-linear due to the Toda potential with a lower dimension, while the oscillator (2) has a low non-linearity with a higher dimension.

In (9b) the coupling is considered by introducing all possible terms of different polynomial order including different products of components of reconstructed state vector of subsystem X on D_a components of the state vector of the subsystem Y, as it was proposed in [9]. In addition, the linear term $c_{Z_j+2}y_{n-l_T}$ is added. In comparison with the linear bivariate model (8) this approach usually leads to better results in detecting a parametric coupling considered in this paper.

4. Numerical experiment

4.1. Unidirectionally coupled oscillators of a same type

In this section pairs of unidirectionally coupled oscillators of a same type were considered: either pairs of subsystems (1) or pairs of subsystems (2). The coupling was investigated in both directions: actual and false.

Two scenarios were considered: for the first one (let us call it *synchronous*) the significant phase synchronisation took place during the stage 2, i.e. $\Phi_{x,y}(t)$ increased significantly in comparison with the stages 1 and 3; the changes in the synchronisation were not detected for the second scenario. For subsystems of both types: (1) and (2) the scenario with the synchronisation increase corresponded to the significant change in dynamics of a driving oscillator: it started to exhibit relatively regular oscillations of a high amplitude and can force the driven oscillator to follow its main rhythm, with driven subsystem being in under-threshold regime of low amplitude oscillations induced by the noise (a stable focal point beneath Andronov–Hopf bifurcation line) for subsystems of type (1) and the self-oscillatory regime of a low amplitude for subsystems of type (2).

In the scenario without any significant synchronisation increase the dynamics of a driving oscillator did not differ in the regime 2 from its dynamics in the regimes 1 and 3. The driven subsystem exhibited a high amplitude oscillations during the stage 2 similar to the synchronised scenario.

For the unidirectionally coupled subsystems of type (1) in the synchronous scenario the linear model showed an increase of $PI(t)$ in both directions: actual and false, i.e. one should say that bidirectional coupling was detected (see Fig. 3(b), grey lines). The surrogate test using the realisations permutation identified this coupling as significant in 10%–20% of cases (one should say that coupling is hard to detect, see Fig. 3(c), grey lines). However, the Fourier components phase randomisation test identified the coupling as significant in more than 80% cases, that should be considered as a coupling presence validation (see Fig. 3(d), grey lines). Both conclusions were incorrect: the permutation test showed an insufficient sensitivity while the Fourier harmonics phase randomisation test showed an insufficient specificity. The surrogates based on Fourier components phase randomisation occurred to be too sensitive to a large phase synchronisation. This is not actually surprising, since the phase randomisation completely broke synchronisation, which led to a large signal distortion. Surrogates of this type occurred to be a good detector of oscillation synchronism irrespective of a reason why this synchronism arose.

The adapted model (9) allowed us to identify the increase of $PI(t)$ in the second stage as significant in the actual direction by means of both surrogate tests (more than 80% of significant results) and the insignificant decrease of $PI(t)$ in the opposite direction (see Fig. 3(b)–(d), black lines). PI decrease may be caused by the fact that large non-linearity is optimal for the individual model (based on BIC criterion $D_s = 2$ and $P = 6$ were chosen), with such highly non-linear model being very well suited especially for the second stage characterised by a more regular dynamics. Therefore the consideration of the second signal occurred to be not so necessary for forecasting.

For the pair of unidirectionally coupled Rössler oscillators in the synchronous regime (see Fig. 4), the linear model showed an increase of PI in the actual direction, with phase randomisation surrogates indicating a coupling in the wrong direction as insignificant and a coupling in the actual one as significant in 40% of cases. The adapted model demonstrated an increase of the coupling only in the actual direction, being significant based on both surrogate tests.

For the pair of unidirectionally coupled Van der Pol-like Toda oscillators for which a synchronisation did not grow significantly during the second stage (see Fig. 5), the linear model showed an increase in the coupling only in the actual direction, however this increase was significant in less than 40% of cases. The adapted model demonstrated the significant increase of PI in the actual direction in 60% cases (surrogates with series permutation) or in 40%

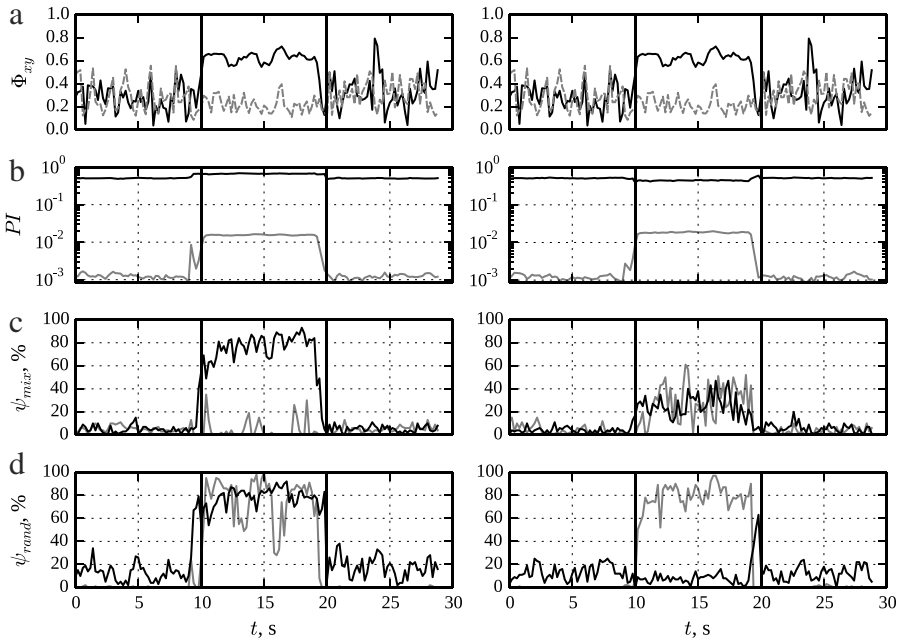

Fig. 3. Coupling detection results for unidirectionally coupled subsystems of the type (1) with the significant phase synchronisation increase in the stage 2: (a) $\Phi_{x,y}(t)$ (black line) and its 95% significance level (grey dashed line); (b)—$PI(t)$; percentage of significant coupling detections with p-value $= 0.05$ based on different surrogate tests: (c) the realisation permutation, (d) the randomisation of phases of Fourier components. Black lines correspond to the adaptive model (9), and grey lines—to the standard linear model (8). Left plots correspond to coupling checking in its actual direction, right—in the opposite (false) one.

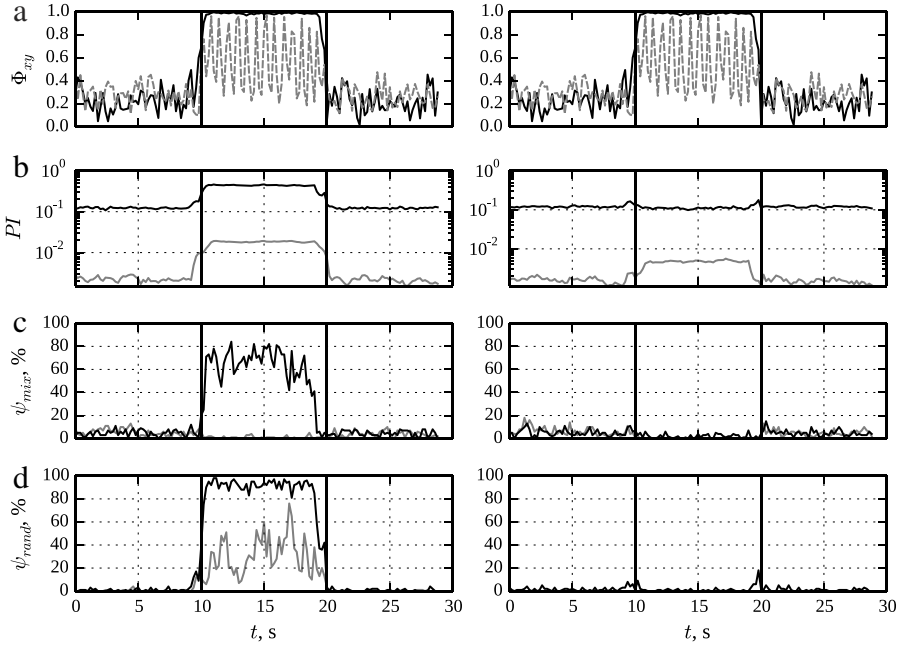

Fig. 4. Coupling detection results for unidirectionally coupled subsystems of the type (2) with the significant phase synchronisation increase in the stage 2: (a) $\Phi_{x,y}(t)$ (black line) and its 95% significance level (grey dashed line); (b)—$PI(t)$; percentage of significant coupling detections with p-value $= 0.05$ based on different surrogate tests: (c) the realisation permutation, (d) the randomisation of phases of Fourier components. Black lines correspond to the adaptive model (9), and grey lines—to the standard linear model (8). Left plots correspond to coupling checking in its actual direction, right—in the opposite (false) one.

(surrogates with randomisation of phases of Fourier components). Also it showed a decrease of *PI* for the stage 2. This can be explained as a result of change in a shape of oscillations: their amplitude increased in 2 or 3 times, but noise variance remained the same in both subsystems, therefore the signal to noise ratio rose, while both prediction errors: ε_s^2 and ε_j^2 fell. However, a more regular signal became simpler for description even by the univariate model, so ε_s^2 fell larger, that can be seen in Fig. 6. Therefore *PI* decreased in the false direction for stage 2, while this effect was compensated in the actual one by the larger rise of *PI* due to the actual increase of the coupling.

Summarising these results with the results obtained previously for subsystems with the significant synchronisation increase (see Fig. 3), the numerical experiments showed the linear model to be likely to work more as a measure of synchrony rather than coupling, since it identified a unidirectional coupling as bidirectional in case of strong synchrony and as absent in case of a weak one. The adapted model in most cases worked better, detecting the coupling in the actual direction and usually considering the coupling in the opposite one as insignificant.

For pairs of unidirectionally coupled Rössler oscillators without any significant synchronisation increase during the stage 2 (Fig. 7)

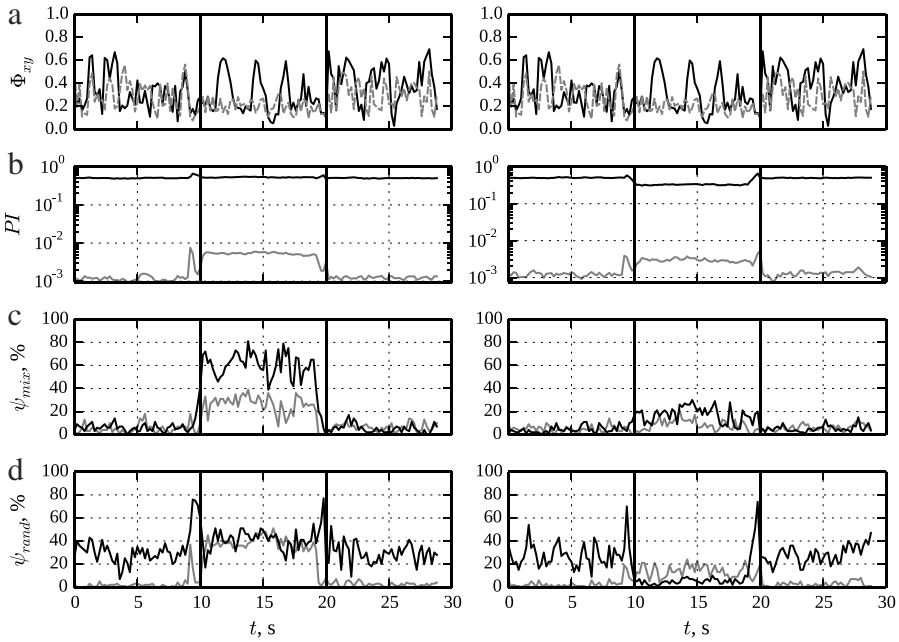

Fig. 5. Coupling detection results for unidirectionally coupled subsystems of the type (1) without the significant phase synchronisation increase in the stage 2: (a) $\Phi_{x,y}(t)$ (black line) and its 95% significance level (grey dashed line); (b)—$PI(t)$; percentage of significant coupling detections with p-value $= 0.05$ based on different surrogate tests: (c) the realisation permutation, (d) the randomisation of phases of Fourier components. Black lines correspond to the adaptive model (9), and grey lines—to the standard linear model (8). Left plots correspond to coupling checking in its actual direction, right—in the opposite (false) one.

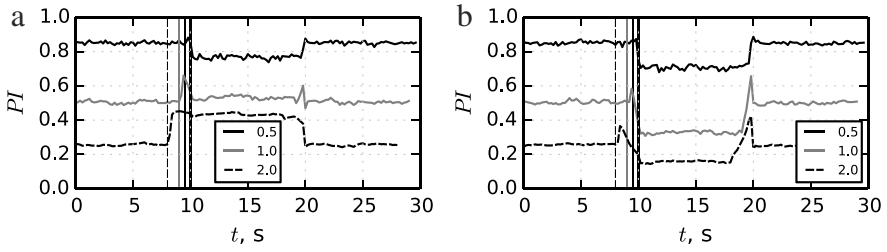

Fig. 6. $PI(t)$ for different lengths of the moving window: the solid black line corresponds to 0.5 s, the grey one corresponds to 1 s, and the dashed black line—to 2 s length. Results are plotted for unidirectionally coupled Van der Pol like-Toda oscillators: (a) in the actual direction, (b) in the false direction.

the linear model indicated a decrease in the coupling in the actual direction and an increase in the false one, i.e. it showed the results, completely opposite to the real coupling architecture. However, these results were insignificant. This confirmed a previous conclusion that the linear model is good for indicating synchrony rather than coupling. The adapted non-linear model demonstrated a good specificity combined with an insufficient sensitivity: it showed no increase of the coupling in the wrong direction during stage 2, but the coupling increase in the actual direction was detected only in 25% of cases. Comparing with previous results a poor performance of the adapted method seems to be mainly a result of lower signal to noise ratio in this regime. Additional numeric experiments showed that sensitivity of the adapted model can be increased either by means of using the longer moving time window (but this leads to a decrease in temporal resolution) or by increasing D_a, but this is very dangerous, since it leads not only to sufficiently larger models, but also provokes false positive results. So, the question of the optimal D_a value remained open.

For most of the considered cases a sharp peak in Granger causality occurs at the start and at the end of the second stage. This effect is caused by a finite length of a moving window in which the model is constructed that can be seen from Fig. 6, where dependencies $PI(t)$ for the same data and a different window length are plotted: for the window of 0.5 s length—with black line, for the window of 1 s length—with grey line, and for the window of 2 s length—with black dashed line. Fig. 6 shows that the wider the window is, the wider is this Granger causality increase at transient processes.

Such an increase of PI can also be explained by the fact that a good forecasting model can hardly be constructed for a transient process due to the non-stationarity. The difficulties of the description of non-autonomous and transient processes using autonomous models were mentioned previously [44,45]. The predictive power of a univariate model based on taking account of values from a modelled series decreases while impact of the second signal remains approximately the same, so the role of an additional term in model (6) rises. Therefore PI jumps up both for a coupling increase and for its decrease (see Fig. 8).

4.2. Unidirectionally coupled oscillators of a different type

The chain of consequently coupled two Van der Pol like-Toda and two Rössler oscillators was studied, with subsystems set in turns: (1) → (2) → (1) → (2). For such a chain the phase synchronisation index $\Phi_{x,y}(t)$ did not show a significant increase in the synchronisation in the stage 2. All three possible pairs of subsystems were considered.

The linear model failed to detect coupling in both directions for all considered pairs as it was in the previous examples, where no synchronisation took place. The adapted model succeeded to

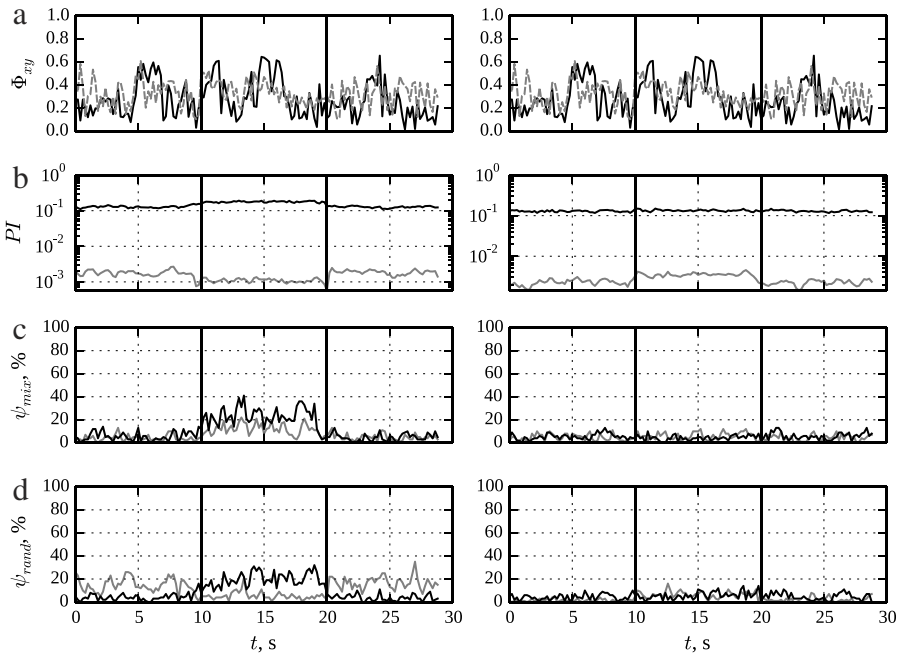

Fig. 7. Coupling detection results for unidirectionally coupled subsystems of the type (2) without the significant phase synchronisation increase in the stage 2: (a) $\Phi_{x,y}(t)$ (black line) and its 95% significance level (grey dashed line); (b)—$PI(t)$; percentage of significant coupling detections with p-value = 0.05 based on different surrogate tests: (c) the realisation permutation, (d) the randomisation of phases of Fourier components. Black lines correspond to the adaptive model (9), and grey lines—to the standard linear model (8). Left plots correspond to coupling checking in its actual direction, right—in the opposite (false) one.

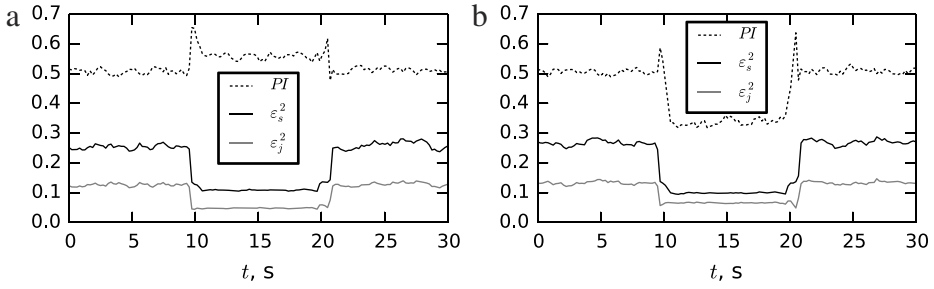

Fig. 8. Dependency of PI, ε_s^2, and ε_j^2 on time for unidirectionally coupled Van der Pol like-Toda oscillators: (a) in the actual direction, (b) in the false direction.

detect the significant coupling in the actual direction in 80% cases based on both surrogate types in the situation when a van der Pol like-Toda oscillator was driving a Rössler oscillator and in 70% (phase randomisation) and 40% (series permutation) cases when a Rössler oscillator drove a van der Pol like-Toda one.

These results showed that even if individual subsystems largely differ one from another, the coupling change nevertheless can be successfully detected with the adapted model, with the linear model being a measure of oscillation synchrony.

Also it is interesting that for the stage 2 the mediated coupling from the first oscillator to the third and fourth ones was not detected (results were mainly insignificant using both types of models and both types of surrogates). This showed that such a coupling should be considered to be too small due to its indirectness that matches the previously mentioned fact that the coupling with $k = 0.01$ was indistinguishable from zero. No doubt that the main reason is the small length of time series and the presence of a large enough noise.

4.3. Bidirectionally coupled oscillators of the same type

For pairs of bidirectionally coupled Van der Pol like-Toda and pairs of bidirectionally coupled Rössler oscillators $PI(t)$ rose in the stage 2. For Van der Pol like-Toda subsystems both models showed approximately the same results, with linear model being not so sensitive (50% cases with both surrogates types) as adapted nonlinear one (more than 80% cases). For Rössler oscillators the results were mainly the same, but the surrogates based on the phase randomisation of Fourier components indicated more results as significant than the surrogates based on the series permutation in the actual direction (see Figs. 9 and 10 left).

In general, the standard linear models occurred to be more efficient for bidirectionally coupled subsystems in comparison with unidirectionally coupled ones, since for bidirectionally coupled systems no false positives were possible (there was no chance to make a mistake in the coupling direction) and the synchrony between subsystems was usually high.

It has to be mentioned that in the considered case two Rössler oscillators demonstrated a delay of ∼1 s between a change of the evolution operator and a change in the amplitude and shape of oscillations (see Fig. 1(a)). However, both types of models detected the regime change immediately when the change of the evolution operator occurred. The same results can be reported for other cases, when two Rössler oscillators were coupled in other manners. This fact is inspiring, since it showed Granger causality to be a perspective tool for revealing actual changes of the evolution operator in complex systems.

4.4. Bidirectionally coupled subsystems of a different type

Pairs of different bidirectionally coupled oscillators: one Van der Pol like-Toda oscillator and one Rössler's oscillator were

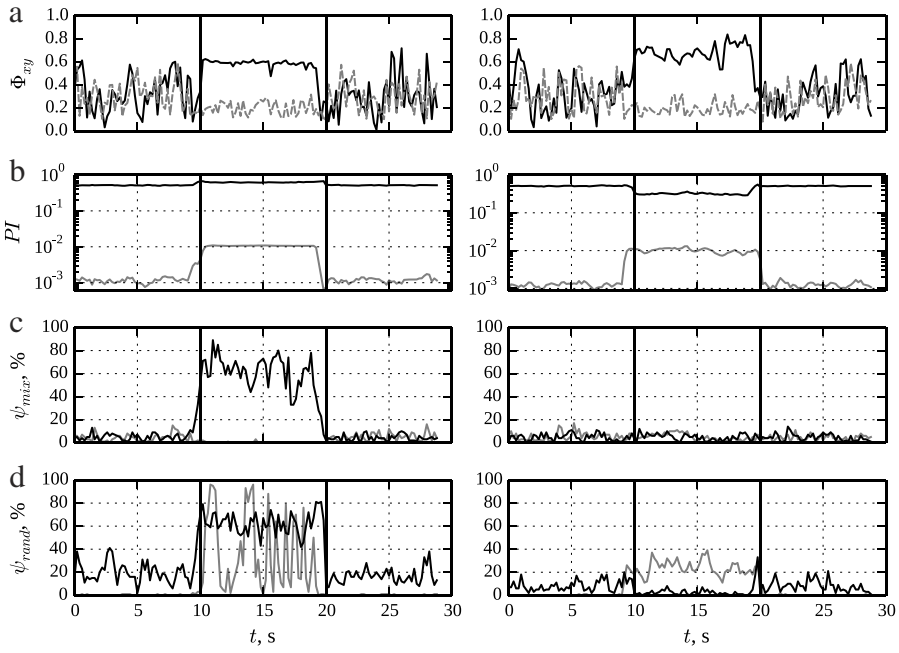

Fig. 9. Coupling detection results for bidirectionally coupled (left) and uncoupled (right) subsystems of the type (1): (a) $\Phi_{x,y}(t)$ (black line) and its 95% significance level (grey dashed line); (b)—$PI(t)$; percentage of significant coupling detections with p-value = 0.05 based on different surrogate tests: (c) the realisation permutation, (d) the randomisation of phases of Fourier components. Black lines correspond to the adaptive model (9), and grey lines—to the standard linear one (8).

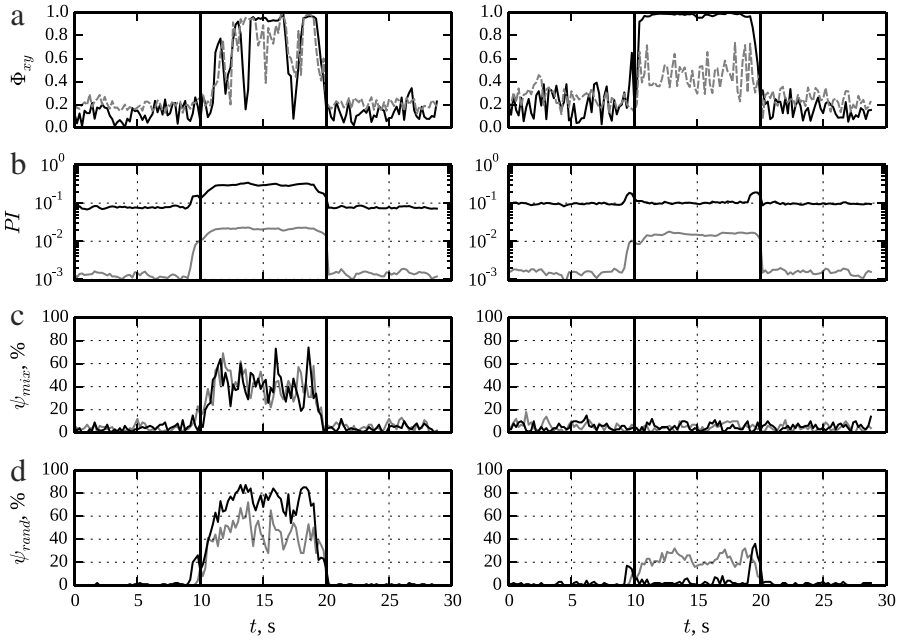

Fig. 10. Coupling detection results for bidirectionally coupled (left) and uncoupled (right) subsystems of the type (2): (a) $\Phi_{x,y}(t)$ (black line) and its 95% significance level (grey dashed line); (b)—$PI(t)$; percentage of significant coupling detections with p-value = 0.05 based on different surrogate tests: (c) the realisation permutation, (d) the randomisation of phases of Fourier components. Black lines correspond to the adaptive model (9), and grey lines—to the standard linear one (8).

considered. $\Phi_{x,y}(t)$ did not rise during the stage 2. The coupling was studied in both directions.

The coupling from a Rössler oscillator to a Van der Pol like-Toda one could hardly be detected and both models with both types of surrogates never gave more than 20% of significant results. *PI* increased for both model types, but for the linear model this increase was more detectable. This was the only case, when the standard linear model performed a little bit better than the adapted one. The coupling in the opposite direction was well detectable with both models. Results of the adapted model were significant in more cases than results of the linear one (40% cases for the standard linear model and 50% cases for the adapted one).

The problems of the adapted model may have different reasons. First, in such a combination Van der Pol like-Toda subsystems were in regime close to the linear one (if the noise was not taken into account), so the non-linear method was not necessary. Also since the noise was dominant in the dynamics, with long correlations being lost, the additional adaptations of the model lag and prediction length values were superfluous, as well as the injection of the second lag l_T. Second, using specialised models of the same type for different oscillators may not be efficient.

Third, the linear model had less coefficients, so they could be estimated more reliably, which became very important in the case of the dominating noise and a short window length. Numerical experiments showed the combination of all these reasons to be able to lead to such poor results, while each of them was not crucial in itself.

4.5. Uncoupled oscillators of the same type

Pairs of uncoupled oscillators of both types (1) and (2) were considered. In order to change a regime in the stage 2, the individual parameters of both subsystems were changed. The achieved regime was very similar to the one obtained by means of increasing the coupling. Due to the small length of the moving time window this led to the significant increase in synchrony during stage 2 in ensembles of subsystems of both types.

Linear models showed an increase in the coupling during the stage 2 for both subsystem types, that was insignificant based on the series permutation surrogates, but significant in 20%–30% cases based on randomisation of phases of Fourier components (see Figs. 9 and 10 right). This indicated one more time that the standard linear Granger causality mainly showed an oscillation synchrony despite its origin, rather than coupling. The non-linear adapted Granger causality indicated *PI* as insignificant for both subsystem types. For Van der Pol like-Toda oscillators *PI* decreased insignificantly that matched the previous results and could be explained similarly (see Section 4.1).

4.6. Uncoupled oscillators of a different type

Uncoupled oscillators of a different type were studied in the same way as uncoupled oscillators of same type. No significant increase of $\Phi_{x,y}(t)$ could be achieved here. Both standard linear and adapted models were shown to work successfully.

5. Conclusion and discussion

First, the standard linear Granger causality is more likely to be a measure of synchrony rather than coupling for the considered types of subsystems and length of the moving window. For most synchronous subsystems it detects the coupling in a wrong direction (bad specificity), and it is not sensitive enough for subsystems with a low level of the synchronisation. The reason why oscillations become synchronous is not very important: the similar results can be achieved for bidirectionally coupled oscillators, for unidirectionally coupled oscillators, and even for uncoupled ones with the close main frequencies (the difference appears to be negligible due to the short length of the used time window).

Second, the adapted non-linear Granger causality is able to benefit from more complex approximating functions, from fitting the prediction length and the embedding lag, as well as from the non-uniform embedding itself. Therefore the adapted method is essentially more applicable than the standard linear one. However, even the adapted method showed too many false positive results for Van der Pol like-Toda oscillators (up to 20% in nonsynchronous regime during the stage 2, when the oscillators of the same type were coupled), whilst demonstrating insufficient sensitivity (only 20%–40% in the synchronous regime, when the oscillators of the same type were coupled) for the other considered object—Rössler oscillators. The insufficient specificity of the method may be explained by the general disadvantage of Granger causality due to finite sampling rate, as was shown in [30]. However, since the large number of false positives occurred mainly when the subsystems of type (1) were considered, the individual properties of signals could also be important. Oscillators of the type (1) have highly non-linear potential, and the large polynomial order $P = 6$ used to approximate this potential in the bivariate model together with the short length of the moving window led to ill conditioned matrices in least-squares routine.

Though the specificity and the sensitivity of the adapted method are not always sufficient, one can use it to detect the reason of the regime change. The mean *PI* and the number of significant *PI* values, estimated based on the realisation permutation technique, rose together for the transition from the stage 1 to the stage 2, if this transition was caused by an actual coupling increase. The mean *PI* and the number of significant *PI* values fell together for the transition from the stage 2 to the stage 3, if this transition was caused by an actual coupling decrease.

Summarising the results obtained for different types of subsystems, different coupling architectures, and different synchrony levels the following answers to the questions formulated in the *Introduction* section can be provided based on the non-linear adapted Granger causality technique:

1. The method is frequently able to detect coupling directionality even using a short time window (1024 points and about only 8 main oscillations). Bidirectional, unidirectional and absent coupling can be distinguished in many cases. However, the specificity and the sensitivity are far from the desired values.
2. The method sensitivity is often insufficient when analysing interactions of subsystems, if the driven subsystem is of type (1). This can be the result of the individual properties of the considered Van der Pol-like Toda oscillator.
3. Different types of surrogates test different hypotheses and their straightforward comparison can be unfair, but since actually they are often used for testing the hypothesis of coupling, some results can be formulated. For the non-linear adapted model surrogates constructed by series permutation were found to be more reliable during the stage 1, while the Fourier phases randomisation based surrogates were more reliable for the stage 2, providing less false positive results.
4. The non-linear adapted method can be applied in case of relatively high values of phase synchronisation index $\Phi_{x,y} = 0.9$. In most cases it also could detect, whether the synchrony was a result of an interaction (unidirectional or bidirectional), or it was caused by a random coincidence of oscillation phases.
5. It is obvious that the method time resolution is mainly defined by moving window length. For considered subsystems, windows of 512, 1024, and 2048 points (from 4 to 16 oscillations) length were considered. Such a time resolution can be considered as high, e.g. in comparison with time resolution of phase based method such as [16], where tens or hundreds of oscillations are mentioned. Moreover, the method was shown to indicate the exact time moment of coupling change, even if the change of the shape and amplitude of oscillations delayed for one window length or larger.
6. Numerical experiments on uncoupled oscillators, where the similar regime changes were established with the change of individual subsystem parameters, showed the adapted non-linear method to be efficient in determining the reason of the observed regime change.

Although the achieved results are to be considered as preliminary and they depend on a large amount of factors such as model dimension, type and number of approximating function, and specifics of the observed signals, these results show that non-linear Granger causality approach is efficient for investigating changes of coupling in time between subsystems in a complex system, even if subsystems are of different nature. To provide this efficiency the carefully adapted models have to be used.

Acknowledgement

This research was funded by the Russian Science Foundation, Grant No. 14-12-00291.

References

[1] L.A. Baccala, K. Sameshima, G. Ballester, A.C. Do Valle, C. Timo-Laria, Studing the interactions between brain structures via directed coherence and Granger causality, Appl. Signal Process. 5 (1998) 40–48.
[2] P. Tass, D. Smirnov, A. Karavaev, U. Barnikol, T. Barnikol, I. Adamchic, C. Hauptmann, N. Pawelcyzk, M. Maarouf, V. Sturm, H.-J. Freund, B. Bezruchko, The causal relationship between subcortical local field potential oscillations and Parkinsonian resting tremor, J. Neural Eng. 7 (2010) 016009.
[3] Boris Gourevitch, Regine Le Bouquin-Jeannes, Gerard Faucon, Linear and non-linear causality between signals: methods, examples and neurophysiological applications, Biol. Cybernet. 95 (2006) 349–369.
[4] Andrea Brovelli, Mingzhou Ding, Anders Ledberg, Yonghong Chen, Richard Nakamura, Steven L. Bressler, Beta oscillations in a large-scale sensorimotor cortical network: Directional influences revealed by Granger causality, PNAS 101 (2004) 9849–9854.
[5] E. Sitnikova, T. Dikanev, D. Smirnov, B. Bezruchko, G. van Luijtelaar, Granger causality: Cortico-thalamic interdependencies during absence seizures in WAG/Rij rats, J. Neurosci. Methods 170 (2008) 245–254.
[6] I.I. Mokhov, D.A. Smirnov, Empirical estimates of the influence of natural and anthropogenic factors on the global surface temperature, Dokl. Earth Sci. 427 (1) (2009) 798–803.
[7] Mokhov, D.A. Smirnov, P.I. Nakonechny, S.S. Kozlenko, E.P. Seleznev, J. Kurths, Alternating mutual influence of El-Niño/southern oscillation and Indian monsoon, Geophys. Res. Lett. 38 (2011) L00F04.
[8] C.W.J. Granger, Investigating causal relations by econometric models and cross-spectral methods, Econometrica 37 (3) (1969) 424–438.
[9] Yonghong Chen, Govindan Rangarajan, Jianfeng Feng, Mingzhou Ding, Analyzing multiple nonlinear time series with extended granger causality, Phys. Lett. A 324 (1) (2004) 26–35.
[10] Daniele Marinazzo, Mario Pellicoro, Sebastiano Stramaglia, Nonlinear parametric model for Granger causality of time series, Phys. Rev. E 73 (2006) 066216.
[11] Daniele Marinazzo, Mario Pellicoro, Sebastiano Stramaglia, Kernel method for nonlinear Granger causality, PRL 100 (2008) 144103.
[12] Thomas Schreiber, Measuring information transfer, Phys. Rev. Lett. 85 (2000) 461.
[13] Luca Faes, Giandomenico Nollo, Alberto Porta, Information-based detection of nonlinear Granger causality in multivariate processes via a nonuniform embedding technique, Phys. Rev. E 83 (2011) 051112.
[14] B. Schelter, J. Timmer, M. Eichler, Assessing the strength of directed influences among neural signals using renormalized partial directed coherence, J. Neurosci. Methods 179 (2009) 121–130.
[15] M. Rosenblum, A. Pikovsky, Detecting direction of coupling in interacting oscillators, Phys. Rev. E 64 (2001) 045202(R).
[16] D. Smirnov, B. Bezruchko, Estimation of interaction strength and direction from short and noisy time series, Phys. Rev. E 68 (2003) 046209.
[17] Lionel Barnett, Adam B. Barrett, Anil K. Seth, Granger causality and transfer entropy are equivalent for Gaussian variables, Phys. Rev. Lett. 103 (2009) 238701.
[18] Wolfram Hesse, Eva Möller, Matthias Arnold, Bärbel Schack, The use of time-variant EEG Granger causality for inspecting directed interdependencies of neural assemblies, J. Neurosci. Methods 124 (2003) 27–44.
[19] Dmitry A. Smirnov, Boris P. Bezruchko, Detection of couplings in ensembles of stochastic oscillators, Phys. Rev. E 79 (2009) 046204.
[20] Jakob Nawrath, M. Carmen Romano, Marco Thiel, István Z. Kiss, Mahesh Wickramasinghe, Jens Timmer, Jürgen Kurths, Björn Schelter, Distinguishing direct from indirect interactions in oscillatory networks with multiple time scales, PRL 104 (2010) 038701.
[21] I.V. Sysoev, M.D. Prokhorov, V.I. Ponomarenko, B.P. Bezruchko, Reconstruction of ensembles of coupled time-delay system from time series, Phys. Rev. E 89 (2014) 062911.
[22] Sebastiano Stramaglia, Jesus M. Cortes, Daniele Marinazzo, Synergy and redundancy in the Granger causal analysis of dynamical networks, New J. Phys. 16 (2014) 105003.
[23] Linda Sommerlade, Marco Thiel, Bettina Platt, Andrea Plano, Gernot Riedel, Celso Grebogi, Jens Timmer, Björn Schelter, Inference of Granger causal time-dependent influences in noisy multivariate time series, J. Neurosci. Methods 203 (2012) 173–185.
[24] Björn Schelter, Malenka Mader, Wolfgang Mader, Linda Sommerlade, Bettina Platt, Ying-Cheng Lai, Celso Grebogi, Marco Thiel, Overarching framework for data-based modelling, Europhys. Lett. EPL 105 (2014) 30004.
[25] B.P. Bezruchko, V.I. Ponomarenko, M.D. Prokhorov, D.A. Smirnov, P.A. Tass, Modeling nonlinear oscillatory systems and diagnostics of coupling between them using chaotic time series analysis: Applications in neurophysiology, Phys. Usp. 51 (2008) 304–310.
[26] G. Schwarz, Estimating the dimension of a model, Ann. Statist. 6 (2) (1978) 461–464.
[27] H. Akaike, A new look at the statistical model identification, IEEE Trans. Automat. Control 19 (1974) 716–723.
[28] Marina V. Sysoeva, Evgenia Sitnikova, Ilya V. Sysoev, Boris P. Bezruchko, Gilles van Luijtelaar, Application of adaptive nonlinear Granger causality: Disclosing network changes before and after absence seizure onset in a genetic rat model, J. Neurosci. Methods 226 (2014) 33–41.
[29] Ilya V. Sysoev, Anatoly S. Karavaev, Pavel I. Nakonechny, Role of model nonlinearity for Granger causality based coupling estimation for pathological tremor, Izv. VUZ Appl. Nonlinear Dyn. 18 (2) (2010) 81–90 (in Russian).
[30] D.A. Smirnov, B.P. Bezruchko, Spurious causalities due to low temporal resolution: Towards detection of bidirectional coupling from time series, Europhys. Lett. 100 (2012) 10005.
[31] Linda Sommerlade, Marco Thiel, Malenka Mader, Wolfgang Mader, Jens Timmer, Bettina Platt, Björn Schelter, Assessing the strength of directed influences among neural signals an approach to noisy data, J. Neurosci. Methods 239 (2015) 47–64.
[32] Marina V. Sysoeva, Taras V. Dikanev, Ilya V. Sysoev, Selecting time scales for empirical model construction, Izv. VUZ Appl. Nonlinear Dyn. 20 (2) (2012) 54–62 (in Russian).
[33] L. Angelini, M. de Tommaso, D. Marinazzo, L. Nitti, M. Pellicoro, S. Stramaglia, Redundant variables and Granger causality, Phys. Rev. E 81 (2010) 037201.
[34] Maxim V. Kornilov, Ilya V. Sysoev, Influence of the choice of the model structure for working capacity of nonlinear Granger causality approach, Izv. VUZ Appl. Nonlinear Dyn. 21 (2) (2013) 74–87 (in Russian).
[35] D. Marinazzo, M. Pellicoro, S. Stramaglia, Kernel–Granger causality and the analysis of dynamical networks, Phys. Rev. E 77 (2008) 056215.
[36] T. Dikanev, D. Smirnov, R. Wennberg, J.L. Perez Velazquez, B. Bezruchko, EEG nonstationarity during intracranially recorded seizures: Statistical and dynamical analysis, Clin. Neurophysiol. 116 (2005) 1796–1807.
[37] J. Theiler, S. Eubank, A. Longtin, B. Galdrikian, J.D. Farmer, Testing for nonlinearity in time series: the method of surrogate data, Physica D 58 (1992) 77–94.
[38] C. Allefeld, J. Kurths, Testing for phase synchronization, Int. J. Bifurcation Chaos 14 (2004) 405–416.
[39] N. Packard, J. Crutchfield, J. Farmer, R. Shaw, Geometry from a time series, Phys. Rev. Lett. 45 (1980) 712–716.
[40] A.M. Legendre, Appendice sur la méthodes des moindres quarrés, in: Nouvelles Méthodes pour la Détermination des Orbites des Comètes, Firmin-Didot, Paris, 1805, (in French).
[41] B. Bezruchko, D. Smirnov, Extracting Knowledge From Time Series, Springer, Berlin, 2010.
[42] M. Sysoeva, I. Sysoev, Mathematical modeling of encephalogram dynamics during epileptic seizure, Tech. Phys. Lett. 38 (2) (2012) 151–154.
[43] K. Judd, A. Mees, Embedding as a modeling problem, Physica D 120 (1998) 273–286.
[44] Boris P. Besruchko, Dmitry A. Smirnov, Constructing nonautonomous differential equations from experimental time series, Phys. Rev. E 63 (2000) 016207.
[45] D.A. Smirnov, I.V. Sysoev, E.P. Seleznev, B.P. Bezruchko, Reconstructing nonautonomous system models with discrete spectrum of external action, Tech. Phys. Lett. 29 (10) (2003) 824–827.